International Journal of Engineering Sciences &Research Technology

(A Peer Reviewed Online Journal)
Impact Factor: 5.164

IJESRT

RESEARCHERID
THOMSON REUTERS

[Chang. *et al.*, 8(9): September, 2019]
IC™ Value: 3.00

ISSN: 2277-9655
Impact Factor: 5.164
CODEN: IJESS7

IJESRT

INTERNATIONAL JOURNAL OF ENGINEERING SCIENCES & RESEARCH TECHNOLOGY

CHARACTERISATION OF GEOMETRIC ERRORS OF A FIVE-AXIS MACHINE TOOL BASED ON LINEAR-ROTARY AXES COORDINATED MOTION

JIANG Xiaogeng[1, 2], YAO Sihan[1, 2], LIU Chang[1, 2, *]

[1.] Tianjin Key Laboratory of Advanced Mechatronics Equipment Technology, Tianjin Polytechnic University, Tianjin, China 300387

[2.] School of Mechanical Engineering, Tianjin Polytechnic University, Tianjin, China 300387

DOI: 10.5281/zenodo.3393445

ABSTRACT

Position Independent Geometric Errors (PIGEs) of rotary axes, which are caused by imperfections during assembly of machine tools, are proved to be a major error source of a five-axis machine tool. In this paper, a PIGEs characterisation method using a Double Ball Bar (DBB) is proposed. The method is used to characterise the PIGEs based on the coordinated motion involving linear and rotary axes of a five-axis machine tool. Based on the machine tool kinematic topological structure and the screw theory, the comprehensive error model of the machine tool is established and the decoupling of PIGEs is realized. This method does not require the definition of local coordinate frames, which greatly simplifies the machine tool modeling process. The DBB is employed as the data sampling tool to capture the error information during the coordinated motion. The PIGEs are calculated based on the machine tool comprehensive error model and simulated with a Matlab program. Using the machine inverse kinematics, the machine tool is compensated for by the error values. The effectiveness of the proposed characterisation method is proved by the compensation results.

Key words: Five-Axis Machine Tool； Geometric Errors； Double Ballbar； Screw Theory

1. INTRODUCTION

Five-axis machine tools are widely used to machine complex geometries [1]. However, the accuracy of machine tool motion is affected by a vast number of errors [2], among which geometric errors are one of the main impact factors [3]. Geometric errors are comprised of Position Dependent Geometric Errors (PDGEs) and Position Independent Geometric Errors (PIGEs) [4, 5]. PDGEs are generated during the movement of the machine tool. Whilst PIGEs stem from faulty assembly of machine components, which cause errors in the position and orientation of the nominal motion trajectories [6]. Also, manufacturing defects in the kinematic parts of a machine tool can result in PIGEs. Therefore, PIGEs are considered to be the predominant influence of machine tool inaccuracy.

To eliminate or reduce the above errors, many researchers have carried out a great number of studies to model and measure the PIGEs. Machine tool error modeling is the process of constructing the mapping relationships between machine tool errors and tool poses, which is the theoretical basis for precision design and error compensation [7]. Common mathematical tools for the expression of tool poses include quaternion, vector differential method, Homogeneous Transformation Matrix (HTMs) [8], multi-body frame method [9], D-H (Denavit-Hartenberg) method based on robot kinematics [10], differential transformation method [11] , neural network method [12], screw theory [13], exponential product formula [15] etc. Compared with the traditional machine tool modeling methods, screw theory modeling has the following advantages. All motion matrices are defined in the machine coordinate frame (MCF), which does not require local framework designation, thus significantly simplifying the modeling process. Screw theory can give a clear analytical solution for the machine tool kinematics, which is capable of machine tool kinematics analysis and error compensation [13,16]. Therefore, this paper uses the screw theory to represent the motion of the linear and rotary axes and their errors.

Many research work has been carried out for the identification of geometric error of five-axis machine tools. Various measuring instruments have been developed for geometric error identification including double ball bar (DBB) [17], R-test [18], Cap ball [19], touch trigger probe [20], and tracking interferometer [21,22]. Among

ISSN: 2277-9655
Impact Factor: 5.164
CODEN: IJESS7

them, the DBB is considered to be an ideal geometric error detection tool because of its short measurement time and simple measurement procedure.

In summary, it is necessary to carry out the coordinated motion experiment between the linear and the rotary axes. Based on this, this paper proposes a serial of experiments and the error decoupling process. The PIGEs of the five-axis machine tool were obtained, and the effectiveness of the decoupling method was verified by comparing the machine tool accuracy before and after compensation.

2. MODELING BY THE SCREW THEORY

2.1 Modeling of kinematic pairs

The basic unit of kinematic modeling based on the screw theory is the screw motions $e^{\hat{\xi}\theta}$. Consider a rigid body moves from one position to another, the kinematic screw motion consists of two sub-movements: a rotation about an axis and a translation along the axis direction. Therefore, each screw motion expression consists of a twists $\boldsymbol{\xi}$ and a motion amount θ. The screw motion is called the twists $\boldsymbol{\xi}$, which describes the instantaneous velocity of the rigid body with linear and angular components [13,16]. Therefore, the twist $\boldsymbol{\xi}$ can be expressed as:

$$\boldsymbol{\xi} = \begin{bmatrix} \mathbf{v} \\ \boldsymbol{\omega} \end{bmatrix}, \mathbf{v} = \mathbf{q} \times \boldsymbol{\omega} \qquad (1)$$

where $\boldsymbol{\omega}$ is the unit vector in the positive direction of the axis of rotation. $\mathbf{q}$ is a random point located on the axis, which is represented in the MCF.

The matrix form of the screw motions of the rotary axis is shown in Eq. 3.

$$e^{\hat{\xi}\theta} = \begin{bmatrix} e^{\hat{\omega}\theta} & \left(\mathbf{I}_{3\times3} - e^{\hat{\omega}\theta}\right)(\boldsymbol{\omega} \times \mathbf{v}) + \boldsymbol{\omega}\boldsymbol{\omega}^{\mathrm{T}}\mathbf{v}\theta \\ 0_{1\times3} & 1 \end{bmatrix} \quad (2)$$

$$e^{\hat{\omega}\theta} = \mathbf{I}_{3\times3} + \hat{\boldsymbol{\omega}} \cdot \sin\theta + \hat{\boldsymbol{\omega}}^2 \cdot (1 - \cos\theta) \qquad (3)$$

where θ is the angle of rotation.

In a five-axis machine tool scenario, a typical example of the C-axis can be given. $\boldsymbol{\omega}$ is $[0 \quad 0 \quad 1]^{\mathrm{T}}$, $\mathbf{q}$ can take a random point on the C-axis. According to the machine structure shown in Figure 1, $\mathbf{q}$ is set to coincide with the origin of the MCF, so $\mathbf{q} = [0 \quad 0 \quad 0]^{\mathrm{T}}$.

Therefore the screw of the C-axis can be given as

$$\begin{aligned} e^{\hat{\omega}_C\theta_C} &= \mathbf{I}_{3\times3} + \hat{\boldsymbol{\omega}}_C \cdot \sin\theta_C + \hat{\boldsymbol{\omega}}_C{}^2 \cdot \ (1 - \cos\theta_C\ ) \\ &= \mathbf{I}_{3\times3} + \begin{bmatrix} 0 & -1 & 0 \\ 1 & 0 & 0 \\ 0 & 0 & 0 \end{bmatrix} \cdot \sin\theta_C \\ &+ \begin{bmatrix} 0 & -1 & 0 \\ 1 & 0 & 0 \\ 0 & 0 & 0 \end{bmatrix}^2 \cdot (1 - \cos\theta_C) \\ &= \begin{bmatrix} \cos\theta_C & -\sin\theta_C & 0 \\ \sin\theta_C & \cos\theta_C & 0 \\ 0 & 0 & 0 \end{bmatrix} \qquad (4) \end{aligned}$$

$$e^{\hat{\xi}_C\theta_C} = \begin{bmatrix} e^{\hat{\omega}_C\theta_C} & \left(\mathbf{I}_{3\times3} - e^{\hat{\omega}_C\theta_C}\right)(\boldsymbol{\omega}_C \times \mathbf{v}) + \boldsymbol{\omega}_C\boldsymbol{\omega}_C{}^{\mathrm{T}}\mathbf{v}\theta_C \\ 0_{1\times3} & 1 \end{bmatrix}$$

$$= \begin{bmatrix} \cos\theta_C & -\sin\theta_C & 0 & 0 \\ \sin\theta_C & \cos\theta_C & 0 & 0 \\ 0 & 0 & 0 & 0 \\ 0 & 0 & 0 & 1 \end{bmatrix} \qquad (5)$$

ISSN: 2277-9655
Impact Factor: 5.164
CODEN: IJESS7

For the linear axes, the matrix form of the screw motions is

$$\xi = \begin{bmatrix} \mathbf{v} \\ 0 \end{bmatrix}, e^{\hat{\xi}\theta} = \begin{bmatrix} \mathbf{I}_{3\times3} & \mathbf{v}\cdot\theta \\ 0_{1\times3} & 1 \end{bmatrix} \qquad (6)$$

where $\mathbf{v}$ is the unit vector in the positive direction of the linear axis motion. θ is the amount of movement of the linear axis. Take the X-axis as an example, the screw motion can be given as

$$\mathrm{v} = \begin{bmatrix} 1 \\ 0 \\ 0 \end{bmatrix}, \theta = x$$

$$e^{\hat{\xi}_X\theta_X} = \begin{bmatrix} \mathbf{I}_{3\times3} & \mathbf{v}_X\cdot\theta_X \\ 0_{1\times3} & 1 \end{bmatrix} = \begin{bmatrix} 1 & 0 & 0 & x \\ 0 & 1 & 0 & 0 \\ 0 & 0 & 1 & 0 \\ 0 & 0 & 0 & 1 \end{bmatrix} \qquad (7)$$

2.2 Error modeling

Based on the screw theory, the modelling process of the geometric errors is established.

The ideal position of the motion of a particular motion axis is P_l. The perfect unit direction vector of the axis is $\boldsymbol{\omega}_l$. However, during the actual movement of the machine tool, due to the geometric error, the axis may move to the actual position P. There is also a angular error θ_e causing rotational deviations. The ideal twists $\boldsymbol{\xi}_l$ and the actual twists $\boldsymbol{\xi}$ expressions are given in Eqs. 8 and 9

$$\boldsymbol{\xi}_l = [\mathbf{q}_l \times \boldsymbol{\omega}_l \quad \boldsymbol{\omega}_l]^{\mathrm{T}} \qquad (8)$$

$$\boldsymbol{\xi} = [\mathbf{q} \times \boldsymbol{\omega} \quad \boldsymbol{\omega}]^{\mathrm{T}} \qquad (9)$$

The deviation from the ideal twists $\boldsymbol{\xi}_l$ to the actual twists $\boldsymbol{\xi}$ can be considered as the result of a helical motion $\hat{\boldsymbol{\xi}}_e\theta_e$, including a rotation around the axis which is perpendicular to the actual axis and the reference axis and a translation of a distance l along the common perpendicular of the actual axis and the reference axis. The parameters θ_e and l are the angular error and position error of the motion axis.

The calculation process of the error twists $\boldsymbol{\xi}_e = [\mathbf{v}_e \quad \boldsymbol{\omega}_e]^{\mathrm{T}}$ is given as:

$$\boldsymbol{\omega}_e = \frac{\boldsymbol{\omega}_l \times \boldsymbol{\omega}}{\sin\theta_e}, h_e = \frac{l}{\theta_e} = \frac{|\mathbf{q} - \mathbf{q}_l|}{\theta_e} \qquad (10)$$

$$\mathbf{v}_e = \frac{\mathbf{q} \times (\boldsymbol{\omega}_l \times \boldsymbol{\omega})}{\sin\theta_e} + h_e \frac{\boldsymbol{\omega}_l \times \boldsymbol{\omega}}{\sin\theta_e} = \frac{\mathbf{q}_l \times \mathbf{q}}{l} + \frac{\mathbf{q} - \mathbf{q}_l}{\theta_e} \qquad (11)$$

When $\theta_e = 0$, the actual axis is parallel to the ideal axis. The error twists describe the position error, which can be expressed as:

$$\boldsymbol{\xi}_e = \begin{bmatrix} \dfrac{\mathbf{q} - \mathbf{q}_l}{\theta_e} \\ 0 \end{bmatrix} \qquad (12)$$

When $l = 0$, the actual axis intersects the ideal axis. The error twists describe the angular error, which can be expressed as:

$$\boldsymbol{\xi}_e = \begin{bmatrix} \mathbf{v} \\ \boldsymbol{\omega} \end{bmatrix} = \begin{bmatrix} \dfrac{\mathbf{q} \times (\boldsymbol{\omega}_l \times \boldsymbol{\omega})}{\sin\theta_e} & \dfrac{\boldsymbol{\omega}_l \times \boldsymbol{\omega}}{\sin\theta_e} \end{bmatrix}^{\mathrm{T}} \qquad (13)$$

The error twists modeling process is illustrated by taking the C-axis as an example. E_{A0C} is orientation error of the C-axis in the A-axis. $\mathbf{q}$ is any point on the C-axis. Therefore, this point is difined at the origin of the C-axis coordinate frame.

In Eqs.10 and 11, $\boldsymbol{\omega}_e$ and $\mathbf{v}_e$ can be expressed as:

$$\boldsymbol{\omega}_e = [0 \quad 1 \quad 0]^{\mathrm{T}} \qquad (14)$$

ISSN: 2277-9655
Impact Factor: 5.164
CODEN: IJESS7

$$\mathbf{v}_e = \mathbf{q} \times \boldsymbol{\omega}_e = \begin{bmatrix} O_{cx} \\ O_{cy} \\ O_{cz} \end{bmatrix} \times \begin{bmatrix} 0 \\ 1 \\ 0 \end{bmatrix} \qquad (15)$$

Then the error twists $\boldsymbol{\xi}_e = [\mathbf{v}_e \quad \boldsymbol{\omega}_e]^{\mathrm{T}}$ is obtained. Other geometric errors can also be modeled by this method.

3.3 **Machine modeling**

In this paper, the experiment is carried out on a DMU 80T five-axis machine. The five-axis machine tool kinematic chain can be divided into two parts: the tool chain and the workpiece chain. The tool chain is the kinematic chain from the tooltip to the MCF, and the workpiece chain is the kinematic chain from the workpiece to the MCF. The positive direction of the motion axis on the tool chain side is set to the right-hand screw in the same direction, and the positive direction of the motion axis on the workpiece chain side is set to the reverse of the right-hand screw [16]. Therefore, for the machine tool structure shown in Figure 2, the two kinematic chains are as shown in Eqs.16 and 17 [16].

$$g_{bt} = e^{\hat{\xi}_X \theta_X} \cdot e^{\hat{\xi}_Y \theta_Y} \cdot e^{\hat{\xi}_B \theta_B} \cdot g_{bt}(0) \qquad (16)$$

$$g_{bw} = e^{-\hat{\xi}_Z \theta_Z} \cdot e^{-\hat{\xi}_C \theta_C} \cdot g_{bw}(0) \qquad (17)$$

where $g_{bw}(0)$ and $g_{bt}(0)$ are the inceptive 4×4 motion matrices of the workpiece and the tool tip relative to the MCF [16].

By premultiplying the error twists, taking the C axis as an example, the PIGEs are expressed as

$$e^{\hat{\xi}_{eC}^I \theta_{eC}^I} \cdot e^{\hat{\xi}_C \theta_C} = e^{\hat{\xi}_{E_{XOC}} E_{XOC}} \cdot e^{\hat{\xi}_{E_{YOC}} E_{YOC}} \cdot e^{\hat{\xi}_{E_{AOC}} E_{AOC}} \cdot e^{\hat{\xi}_{E_{BOC}} E_{BOC}} \cdot e^{\hat{\xi}_C \theta_C} \qquad (17)$$

Combine the Eqs.16 and 17, the PIGEs error model of the five-axis machine tool are given as Eqs.18,19 and 20.

$$g_{bt}^e = (e^{\hat{\xi}_{eX}^I \theta_{eX}^I} \cdot e^{\hat{\xi}_X \theta_X}) \cdot (e^{\hat{\xi}_{eY}^I \theta_{eY}^I} \cdot e^{\hat{\xi}_Y \theta_Y}) \cdot (e^{\hat{\xi}_{eB}^I \theta_{eB}^I} \cdot e^{\hat{\xi}_B \theta_B}) \cdot g_{bt}(0) \qquad (18)$$

$$g_{bw}^e = (e^{\hat{\xi}_{eZ}^I \theta_{eZ}^I} \cdot e^{-\hat{\xi}_Z \theta_Z}) \cdot (e^{\hat{\xi}_{eC}^I \theta_{eC}^I} \cdot e^{-\hat{\xi}_C \theta_C}) \cdot g_{bw}(0) \qquad (19)$$

$$g_{wt}^e = g_{wb}^e \cdot g_{bt}^e = (g_{bw}^e)^{-1} \cdot g_{bt}^e \qquad (20)$$

It should be noted that this modeling method is equally applicable to the other two five-axis machine structures.

3. EXPERIMENTAL DESIGN

According to the structure of the DMU 80T machine tool, the linkage experiment between X-axis and C-axis is designed. According to the X-axis stroke of the machine tool, the DBB with 50mm extension bar is selected. In the experiment, the X-axis performs a linear motion of +250-+50, and the C-axis performs a rotary motion of 0°-360°. As shown in Figure 1, the MCF is defined on the axis-line of C-axis.

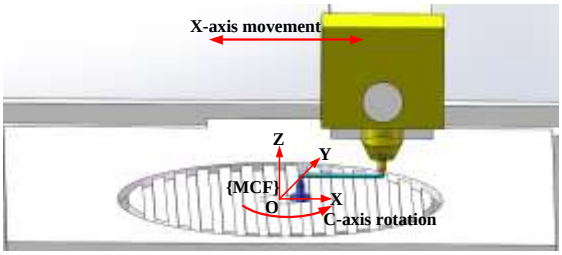

Fig.1 X-axis and C-axis linkage experiment

In order to ensure that the length of the DBB is constant, the connection between the X-axis displacement X and the C-axis rotation angle θ_C is given as Eq.21.

ISSN: 2277-9655
Impact Factor: 5.164
CODEN: IJESS7

$$X = \sqrt{150^2 - (100\sin\theta_C)^2} + 100\cos\theta_C \quad (21)$$

Using the screw theory, the trajectory of the tool tip point relative to the workpiece coordinate frame during the experiment is modeled to obtain the motion trajectory.

$$g_{wt} = (e^{-\hat{\xi}_Z\theta_Z} \cdot e^{-\hat{\xi}_C\theta_C} \cdot g_{bw}(0))^{-1} \cdot e^{\hat{\xi}_X\theta_X} \cdot e^{\hat{\xi}_Y\theta_Y} \cdot e^{\hat{\xi}_B\theta_B} \cdot g_{bt}(0) \quad (22)$$

Among them, because the X-axis and C-axis motions are involved in the experiment, the matrix forms of the Y-axis rotation $e^{\hat{\xi}_Y\theta_Y}$, the B-axis rotation $e^{\hat{\xi}_B\theta_B}$ and the Z-axis rotation $e^{-\hat{\xi}_Z\theta_Z}$ are all unit matrices. The matrix form of the X-axis rotation and the C-axis rotation is expressed as:

$$e^{\hat{\xi}_C\theta_C} = \begin{bmatrix} \cos\theta_C & -\sin\theta_C & 0 & 0 \\ \sin\theta_C & \cos\theta_C & 0 & 0 \\ 0 & 0 & 1 & 0 \\ 0 & 0 & 0 & 1 \end{bmatrix}$$

$$e^{\hat{\xi}_X\theta_X} = \begin{bmatrix} 1 & 0 & 0 & X \\ 0 & 1 & 0 & 0 \\ 0 & 0 & 1 & 0 \\ 0 & 0 & 0 & 1 \end{bmatrix}$$

$$g_{bt}(0) = \begin{bmatrix} 1 & 0 & 0 & 100 \\ 0 & 1 & 0 & 0 \\ 0 & 0 & 1 & 100 \\ 0 & 0 & 0 & 1 \end{bmatrix}$$

$$g_{bw}(0) = \begin{bmatrix} 1 & 0 & 0 & 250 \\ 0 & 1 & 0 & 0 \\ 0 & 0 & 1 & 100 \\ 0 & 0 & 0 & 1 \end{bmatrix} \quad (23)$$

The position of the tool tip point relative to the workpiece coordinate frame is given as:

$$g_{wt} \cdot \begin{bmatrix} 0 \\ 0 \\ 0 \\ 1 \end{bmatrix} = \begin{bmatrix} 250\cos\theta_C + X\cos\theta_C - 100 \\ X\sin\theta_C + 250\sin\theta_C \\ 0 \\ 1 \end{bmatrix} \quad (24)$$

To achieve an accurate record of the DBB, the X-axis and the C-axis is moved at the same time. Therefore, the two-axis motion is realized by equally dividing the X-axis and the C-axis by the trajectory.

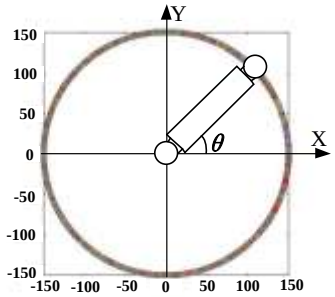

Fig.2 X-axis and C-axis linkage trajectory

As shown in Figure 2, the simulated trajectory is a circle, which is equally divided according to the angle. The coordinate of the equidistant points to the angle θ should be $(150\cos\theta,\ 150\sin\theta)$. At the same time, the coordinates of the equidistant points are $(250\cos\theta_C + X\cos\theta_C - 100,\ X\sin\theta_C + 250\sin\theta_C)$.

$$\begin{cases} 150\cos\theta = 250\cos\theta_C + X\cos\theta_C - 100 \\ 150\sin\theta = X\sin\theta_C + 250\sin\theta_C \end{cases} \quad (25)$$

The connection between θ and θ_C is established, then calculating the θ_C which is corresponded to the equidistant points, and the X coordinate is obtained.

ISSN: 2277-9655
Impact Factor: 5.164
CODEN: IJESS7

$$\cot\theta_C = -\frac{150\cos\theta + 100}{150\sin\theta} \qquad (26)$$

Through the formula, the connection between the linkage trajectory angle and the C-axis rotation angle is obtained. According to this, the G code can realize the uniform motion of the X-axis and the C-axis.

4. EXPERIMENTAL ENVIRONMENT

Calibrating the DBB spindle tool cup and the pivot tool cup. Place the base of the DBB on the centimeter, and use the probe to detect the position of the DBB pivot on the C axis 0°, X-axis +100, Y-axis +0 position. If the position deviates, it can be corrected by adjusting the platform. The spindle tool cup is tested with a dial gauge to ensure accurate and reliable experimental results.

5. EXPERIMENT RESULTS AND DISCUSSION

The six PIGEs included in the X-axis and C-axis experiments were decoupled by the experiment results shown in Figure 3.a , which is from the X-axis and C-axis experiments.

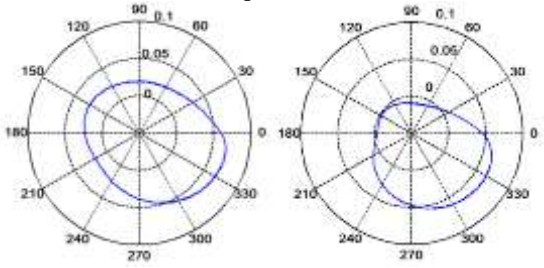

a ***b***

Fig.3 experimental data (a the X-axis and C-axis, b the Y-axis and C-axis)

During the experiment, only the X-axis and C-axis motions， and there are total six PIGEs which involved in XC linkage experiment.

$$g_{wt}^{e} = (e^{\hat{\xi}_{eC}^{I}\theta_{eC}^{I}} \cdot e^{-\hat{\xi}_{C}\theta_{C}}) \cdot g_{bw}(0))^{-1} \cdot (e^{\hat{\xi}_{eX}^{I}\theta_{eX}^{I}} \cdot e^{\hat{\xi}_{X}\theta_{X}} \cdot g_{bt}(0)) \qquad (27)$$

$$L_{DBB} = \| g_{wt}^{e} \cdot [0 \quad 0 \quad 0 \quad 1]^{T} \| \qquad (28)$$

L_{DBB} is the length data measured by the DBB.

By substituting the length data measured by the DBB, an overdetermined equation group can be constructed. Using the pseudo inverse function, the over determined equations are solved, then the six PIGEs in the XC linkage expreriment are obtained.

Similarly, the YC linkage experiment can also be performed by the above method. Using the screw theory, the YC linkage expreriment modeling is established.

$$g_{wt}^{e} = (e^{\hat{\xi}_{eC}^{I}\theta_{eC}^{I}} \cdot e^{-\hat{\xi}_{C}\theta_{C}}) \cdot g_{bw}(0))^{-1} \cdot (e^{\hat{\xi}_{eY}^{I}\theta_{eY}^{I}} \cdot e^{\hat{\xi}_{Y}\theta_{Y}} \cdot g_{bt}(0)) \qquad (29)$$

The results of the YC linkage experiment are shown in Figure 10.b. Then the six PIGEs is decoupled, which are included in the YC linkage experiment.

Through decoupling, the author obtained six PIGEs values in the XC, YC linkage experiments, as shown in Table 2.

ISSN: 2277-9655
Impact Factor: 5.164
CODEN: IJESS7

Table 2 PIGEs values

XC		YC	
PIGEs	Values	PIGEs	Values
E_{X0C}(μm)	32.35	E_{X0C}(μm)	35.95
E_{Y0C}(μm)	47.69	E_{Y0C}(μm)	52.27
E_{A0C}(μrad)	-5.2	E_{A0C}(μrad)	-4.1
E_{B0C}(μrad)	-1.6	E_{B0C}(μrad)	-2.3
E_{B0X}(μrad)	1.6	E_{A0Y}(μrad)	2.3
E_{C0X}(μrad)	21.6	E_{C0Y}(μrad)	19

In the XC and YC linkage experiments, the C-axis motion is involved simultaneously, and both can detect the C-axis PIGEs values. Because the XC and YC experiment are affected by factors such as machine temperature [23-25], the measured C-axis PIGEs values are slightly different. The deviation is shown in Figure 4.

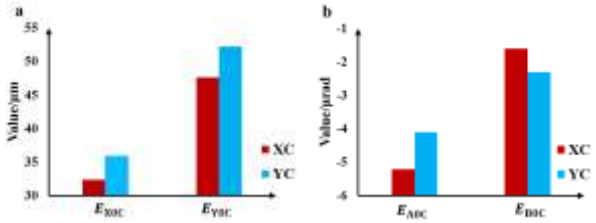

Fig.4 C-axis PIGEs deviation (a position error, b orientation error)

The decoupled PIGEs values are put into the machine model to compensate the machine tool error.

6. CONCLUSIONS

The five-axis machine tool PIGEs model was constructed using the screw theory. Experiments on the linkage between the rotary axes and the linear axes, through the mathematical model, make the linear axis and the rotary axis move at a constant speed. The PIGEs in the two-axis linkage experiment were decoupled and compensated by the decoupled PIGEs. The effectiveness of the decoupling method is verified by paying the front and rear rod length data. The proposed error detection method provides a new and efficient detection method for the periodic inspection of machine tools.

7. ACKNOWLEDGEMENT

This work is supported by the Science & Technology Development Fund of Tianjin Education Commission for Higher Education (2017KJ079).

REFERENCES

[1] Moriwaki T. Multi-functional machine tool[J]. CIRP Annals-Manufacturing Technology, 2007, 57(2): 736-749.
[2] Schwenke H, Knapp W, Haitjema H et al. Geometric error measurement and compensation of machines-an update[J]. CIRP Annals-Manufacturing Technology, 2008, 57(2): 660-675.
[3] Ramesh R, Mannan MA, POO AN. Error composition in machine tools–a review part I; geometric, cutting-force induced and fixture-dependent errors[J]. International Journal of Machine Tools and Manufacture, 2000, 40(9): 1235-1256.
[4] Lee KI, Yang SH. Robust measure method and uncertainty analysis for position-independent geometric errors of a rotary axis using a double ball-bar[J]. International Journal of Precision Engineering and Manufacturing, 2013, 14(2): 231-239.
[5] ISO 230-1, Test Code for Machine Tools Part1:Geometric accuracy of Machines Operating under No-load or Quasi -static Conditions[S]. ISO, 2012.
[6] Jiang X, Cripps, R. J. Accuracy evaluation of rotary axes of five-axis machine tools with a single setup of a double ball bar[J]. Proceedings of the Institution of Mechanical Engineers, Part B: Journal of Engineering Manufacture, 2017, 231(3): 427-436.

ISSN: 2277-9655
Impact Factor: 5.164
CODEN: IJESS7

[7] Li J, Xie F, Liu X et al. Analysis on the research status of volumetric positioning accuracy improvement methods for five-axis NC machine tools[J]. Chinese Journal of Mechanical Engineering, 2017, 53(7):113-128.
[8] Jiang X, Cripps RJ. Geometric characterisation and simulation of position independent geometric errors of five-axis machine tools using a double ball bar[J]. International Journal of Advanced Manufacturing Technology, 2016, 83:1905-1915.
[9] Chen D, Fan J, Zhang F. Extraction the unbalance features of twistsdle frame using wavelet transform and power spectral density[J]. Measurement,2013,46(3) : 1279-1290.
[10] Psang D, Chian S. Modeling and measurement of active parameters and workpiece home position of a multi-axis machine tool[J]. International Journal of Machine Tools and Manufacture, 2008, 48 : 338-349.
[11] Chen J, Lin S, He B. Geometric error compensation for multi-axis CNC machines based on differential transformation[J]. International Journal of Advanced Manufacturing Technology, 2014, 71 : 635-642.
[12] Tan K, Huang S, Lee T. Geometrical error compensation and control of an XY table using neural networks[J]. Control Engineering Practice, 2006, 14: 59-69.
[13] Yang J, Mayer J, Altintas Y. A position independent geometric errors identification and correction method for five-axis serial machines based on screw theory [J]. International Journal of Machine Tools and Manufacture, 2015, 95 : 52-66.
[14] Hsu Y, Wang S. A New Compensation Method for Geometry Errors of Five-axis Machine Tools. International Journal of Machine Tools and Manufacture, 2007, 47: 352-360.
[15] Fu G, Fu J, Xu Y et al. Product of exponential model for geometric error integration of multi-axis machine tools. The International Journal of Advanced Manufacturing Technology, 2014, 71:1653-1667.
[16] Xiang S, Altintas Y. Modeling and compensation of volumetric errors for five-axis machine tools. International Journal of Machine Tools and Manufacture, 2016, 75: 559-572.
[17] Xia H, Peng W, Ouyang X et al. Identification of geometric errors of rotary axis on multi-axis machine tool based on kinematic analysis method using double ball bar[J]. International Journal of Machine Tools and Manufacture, 2017,122: 161-175.
[18] Weikert, S., Knapp, W. R-test, a New Device for Accuracy Measurements on Five Axis Machine Tools[J]. CIRP Annals-Manufacturing Technology, 2004, 53: 429-432.
[19] Zargarbashi S, Mayer, J. Single Setup Estimation of a Five-axis Machine Tool Eight Link Errors by Programmed Endpoint Constraint and on the Fly Measurement with Cap Ball Sensor[J]. International Journal of Machine Tools and Manufacture, 2009,49(10): 759-766.
[20] Givi M, Mayer J. Validation of volumetric error compensation for a five-axis machine using surface mismatch producing tests and on-machine touch probing[J]. International Journal of Machine Tools & Manufacture, 2014.87: 89–95.
[21] Ibaraki S, Ota Y. A machining test to calibrate rotary axis error motions of five-axis machine tools and its application to thermal deformation test[J]. International Journal of Machine Tools & Manufacture , 2014, 86: 81–88.
[22] Ibaraki S, Kudo T, Yano T et al. Estimation of three-dimensional volumetric errors of machining centers by a tracking inter-ferometer[J]. Precision Engineering. 2015,39: 179–186.
[23] Xiang S, Yao X, Du Z et al. Dynamic linearization modeling approach for twistsdle thermal errors of machine tools[J]. Mechatronics,2018,53:215-228.
[24] Wiessner M, Blaser P, Bohl S et al. Thermal test piece for 5-axis machine tools[J]. Precision Engineering, 2018,52:407-417.
[25] Blaser P, Pavlicek F, Mori K et al. Adaptive learning control for thermal error compensation of 5-axis machine tools[J]. Journal of Manufacturing Frames, 2017, 44(2): 302-309.